SUPPLEMENTARY INFORMATION

STRUCTURAL MODELING, *IN VITRO* ANTIPROLIFERATIVE ACTIVITY AND EFFECT OF SUBSTITUENTS ON DNA FASTENING AND SCISSION ACTIONS OF HETEROLEPTIC COPPER(II) COMPLEXES WITH TERPYRIDINES AND NAPROXEN DRUG

Dharmasivam Mahendiran[a], Perumal Gurumoorthy[a], Krishnasamy Gunasekaran[b], Raju Senthil Kumar[c], Aziz Kalilur Rahiman[a*]

[a]*Post-Graduate and Research Department of Chemistry, The New College (Autonomous), Chennai-600 014, India*

[b]*CAS in Crystallograph and Bioinformatics, University of Madras, Guindy Campus, Chennai-600 025, India*

[c]*Department of Pharmaceutical Chemistry, Swami Vivekanandha College of Pharmacy, Elayampalayam, Tiruchengodu-637 205, India*

---

1. Frontier molecular orbital properties of complexes 1 and 6

For complex **1**, the first five HOMOs (from HOMO to HOMO–4) show main contributions from the Cu(II) center and minor percentage from terpyridine and naproxen ligands. As shown in **Fig. S4**, the three highest HOMOs (HOMO, HOMO–2, and HOMO-3) correspond to t_{2g} (Cu) orbitals (d_{xy}, d_{xz}, and d_{yz}), while HOMO–1 and HOMO–4 correspond to e_g (Cu) orbitals ($d_{x^2-y^2}$ and d_{z^2}). Obviously, the degeneracy of the five (Cu) d orbitals is distorted in **1** rather than the idealized degeneracies of three t_{2g} and two e_g levels. The longest wavelength bands at 563.6 and 553.5 nm can be attributed to the transitions of d→d character, and moderately intense band appeared at 411.9 nm is assigned to ligand-metal charge transfer (π(nap)→d/π*(ttpy)) transitions, whereas the 274.3 and 239.3 nm mainly from the ligand–ligand charge transfer and inter–ligand (IL) transitions (π(nap)→π*(ttpy)/π*(nap)) (**Table S2**).

The first six lowest LUMOs of complex **1** (from LUMO to LUMO+5), due to the symmetrical character of the structure (**Fig. S4**), fall in three sets of orbitals with same energy level, LUMO/LUMO+1, LUMO+2/LUMO+3, and LUMO+4/LUMO+5. LUMO to

LUMO+3 show main contributions from the Cu(II) center and minor percentage of contribution from terpyridine ligands, but LUMO+4 and LUMO+5 show main contributions from the terpyridine and minor percentage from naproxen ligand. The LUMO/LUMO+1 orbitals, lying –1.72 eV, and other set of energy level LUMO+2/LUMO+3 and LUMO +4/LUMO+5, are calculated to be –0.89 and –0.56 eV higher in energy than that of LUMO/LUMO+1.

In case of complex **6**, the HOMO is constituted 43% L^6, 12% naproxen and 42% copper characteristics, and the LUMO has 96% contribution from L^6. So, the HOMO to LUMO transition may be assigned to the admixture of naproxen→terpyridine and Cu(dπ) →L(π*). Based on these observations, the terpyridine ligands play significant role in the virtual frontier and in the lower occupied molecular orbitals in both complexes.

Table S1 B3LYP/6-31G(d) Bond Lengths (Å) and Bond Angles (°) of complexes 1, 2, 5 and 6

	Calculated				Experimental	
Complexes	**1**	**2**	**5**	**6**	**1**	**6**
bond length Å						
N(1)-Cu(1)	2.0231	2.0298	2.0389	2.0353	2.087(10)	2.033(6)
N(2)-Cu(1)	1.9290	1.9311	1.9210	1.9365	1.939(10)	1.949(6)
N(3)-Cu(1)	2.0198	2.0443	2.0361	2.0291	2.080(10)	2.059(6)
O(1)-Cu(1)	1.9274	1.9432	1.9343	1.9201	1.948(10)	1.921(5)
O(2)-Cu(1)	2.8009	2.5391	2.6352	2.7321	2.654(10)	2.5824(5)
Cu(1)-Cl(1)	2.3861	2.5900	2.556	2.456	2.427(4)	2.518(2)
bond angle (deg)						
O(2)-Cu(1)-N(2)	164.34	157.92	162.88	160.54	152.7(4)	166.8(2)
O(2)-Cu(1)-N(1)	100.18	93.40	92.76	83.08	78.7(4)	99.4(2)
N(2)-Cu(1)-N(1)	80.87	90.22	88.49	80.42	98.6(4)	79.5(3)
O(2)-Cu(1)-N(3)	103.48	98.19	104.54	108.99	79.4(4)	99.2(2)
N(2)-Cu(1)-N(3)	81.12	78.69	89.73	80.73	98.8(4)	79.0(2)
N(1)-Cu(1)-N(3)	150.30	145.05	151.65	148.05	157.7(4)	156.1(2)
O(2)-Cu(1)-Cl(1)	112.8	105.54	98.04	97.54	110.5(3)	96.46(17)
N(2)-Cu(1)-Cl(1)	94.65	94.10	97.80	96.10	96.8(3)	96.71(18)
N(1)-Cu(1)-Cl(1)	100.02	99.87	97.19	98.34	98.2(3)	96.80(18)
N(3)-Cu(1)-Cl(1)	97.05	91.06	90.62	94.87	93.6(3)	95.92(17)

Table S2 The energy of experimental absorption bands and the electronic transitions calculated with the TD–DFT method for complex 1

The most important orbital excitations	Major contributions	E (eV)	λ (nm) (cal)	f	λ (nm) (exp)
HOMO → LUMO	d → d/π*(ttpy)	2.20	563.6	0.0012	612,
HOMO → LUMO+1	d → d/π*(ttpy)	2.24	553.5	0.0026	562,
HOMO → LUMO+2	π (ttpy) → π*(ttpy) /d	3.01	411.9	0.0043	412,
HOMO-1 → LUMO+1	π(nap) → π*(ttpy) /d	3.44	360.4	0.0096	372
HOMO–2 → LUMO	d → π*(ttpy)/d	3.73	332.4	0.0237	343
HOMO–2 → LUMO+1	d → π*(ttpy)/d	3.77	328.9	0.0253	
HOMO–1 → LUMO	π(nap) → π*(ttpy)/d	3.97	312.3	0.0216	
HOMO–4 → LUMO	π(nap) → π*(ttpy)/d	4.10	302.4	0.0514	
HOMO–3 → LUMO+1	d → π*(ttpy) /d	4.10	302.4	0.0514	
HOMO–4 → LUMO+1	π(nap) → π*(ttpy)/d	4.14	299.5	0.0560	
HOMO–1 → LUMO+3	π(nap) → π*(ttpy)/d	4.31	287.7	0.0379	
HOMO–1 → LUMO+4	π(nap) →π*(ttpy)/π*(nap)	4.52	274.3	0.0712	275
HOMO–3 → LUMO	d → π*(ttpy)/d	4.60	269.5	0.0578	
HOMO–1 → LUMO+5	π(nap) →π*(ttpy)/π*(nap)	4.63	267.8	0.0884	
HOMO–4 → LUMO+2	π(nap) → π*(ttpy)/d	4.91	252	0.0186	
HOMO–2 → LOMO+5	d → π*(nap)/π*(ttpy)	4.96	250	0.0300	
HOMO–3 → LUMO+4	d → π*(ttpy)/π*(nap)	5.18	239.3	0.0611	
HOMO–4 → LOMO+5	π(nap) →π*(nap)/π*(ttpy)	5.33	232.6	0.1512	229

f → Oscillator strength

Table S3 Electrochemical parameters for complexes 1–6

Complexes	i_{pc} (10^{-5} A)	E_{pc} (V)
1	2.01	–0.765
2	1.53	–0.768
3	2.03	–0.759
4	1.35	–0.751
5	1.76	–0.825
6	2.06	–0.818

Table S4 Electrochemical parameters for complexes 1–4 in the absence and presence of CT-DNA

Complexes	R	i_{pc} (10^{-5} A)	E_{pc} (V)
1	0	1.76	–0.765
	1	1.45	–0.754
5	0	2.01	–0.825
	1	1.23	–0.769
6	0	2.06	–0.818
	1	1.98	–0.786

Table S5 Effect of complexes 1 and 5 on apoptosis of MCF–7 cells by Hoechst dye staining method

Drug Treatment	Apoptosis (%)
Control	7.8 ± 0.81
Complex–1 (25 μM)	29.6 ± 1.21
Complex–1 (50 μM)	59.7 ± 1.2
Complex–5 (25 μM)	37.6 ± 3.48
Complex–5 (50 μM)	67.3 ± 1.12

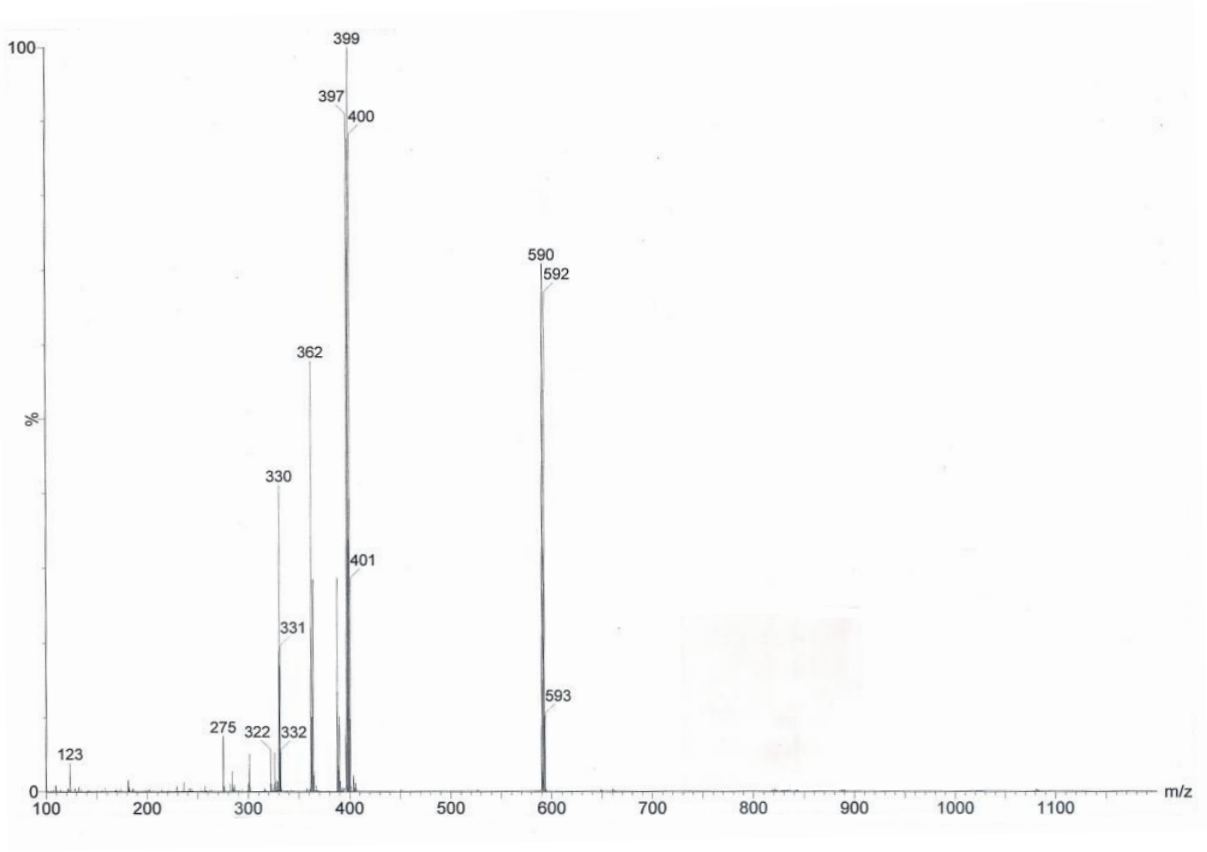

Fig. S1 ESI mass spectrum of complex 6.

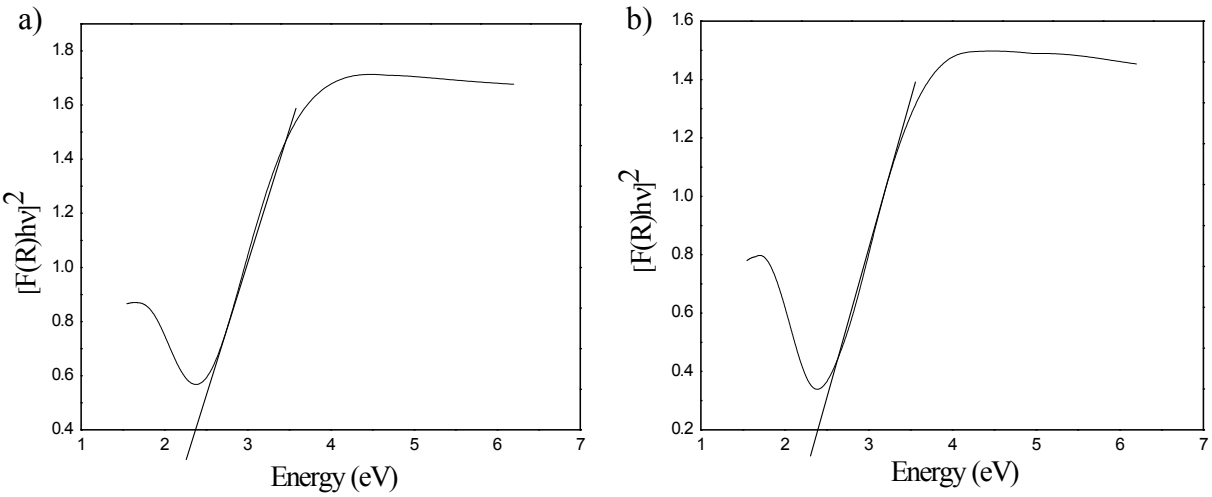

Fig. S2 Determination of the band-gap energy for complexes 1 (a) and 5 (b) from diffuse reflectance measurements.

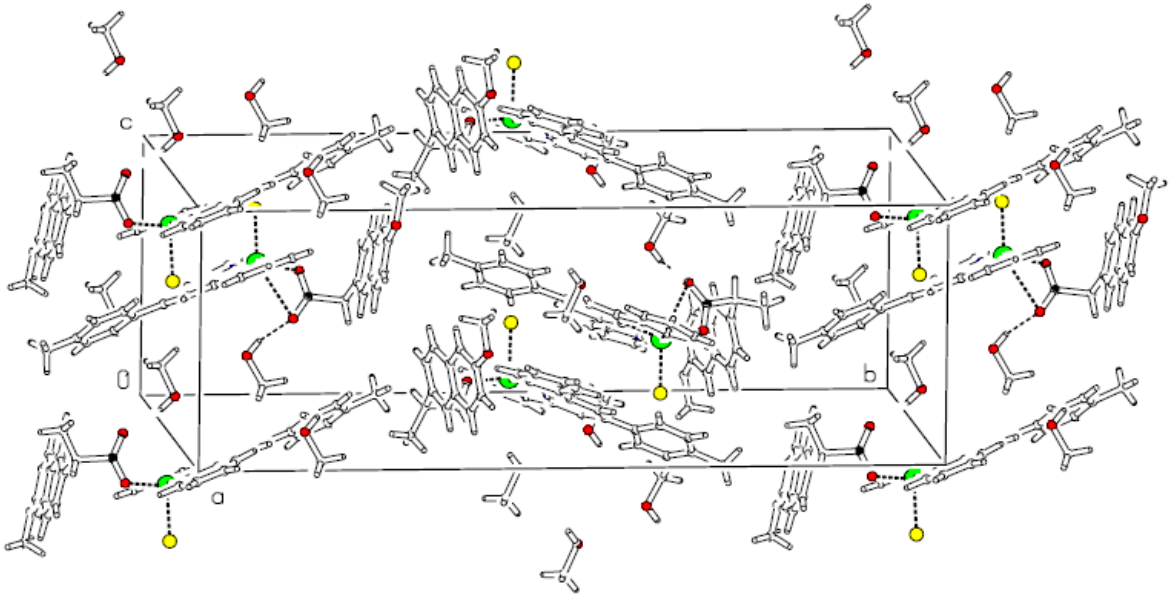

Fig. S3 Unit cell packing diagram of complex 1.

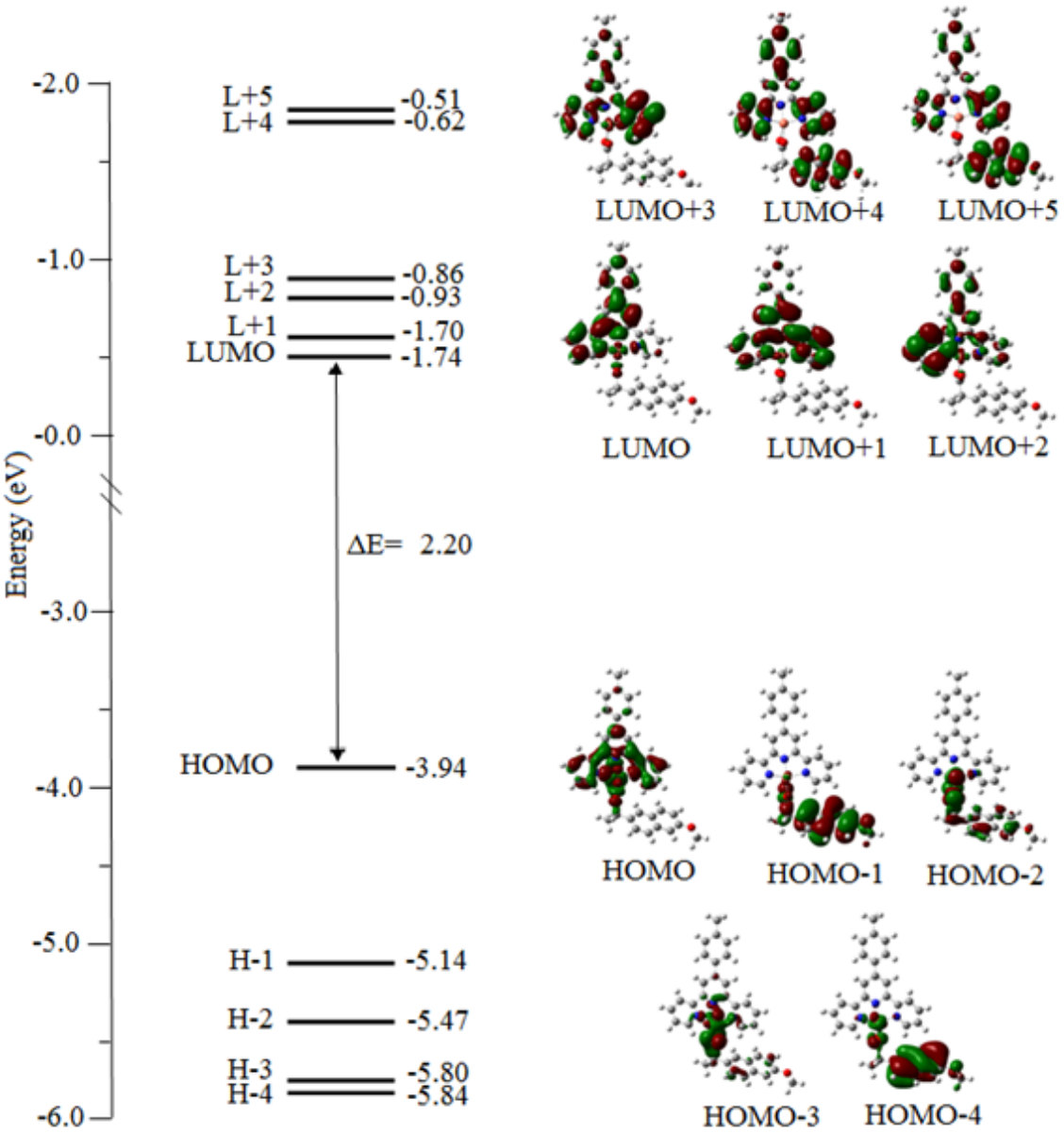

Fig. S4 Frontier MOs of complex 1.

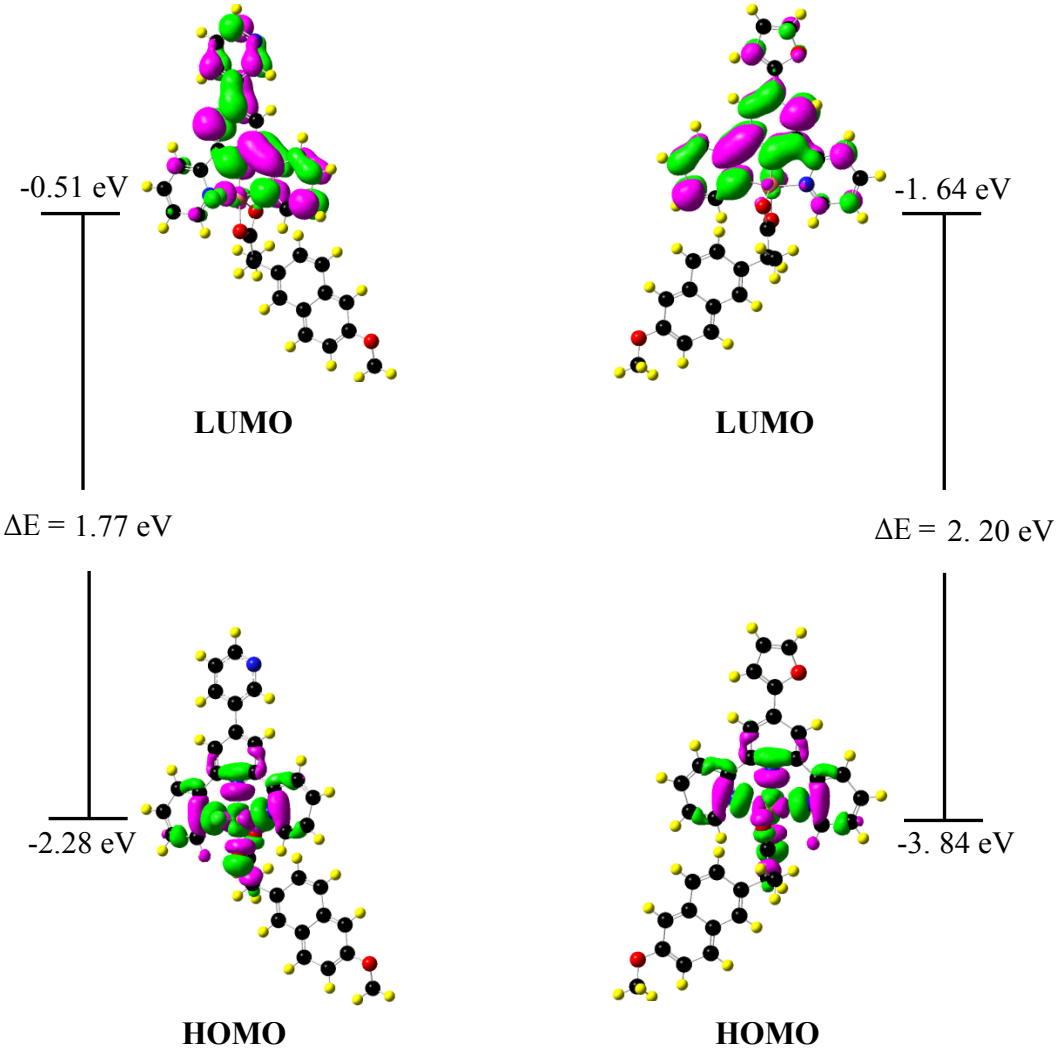

Fig. S5 Frontier molecular orbital of the complexes 5 and 6.

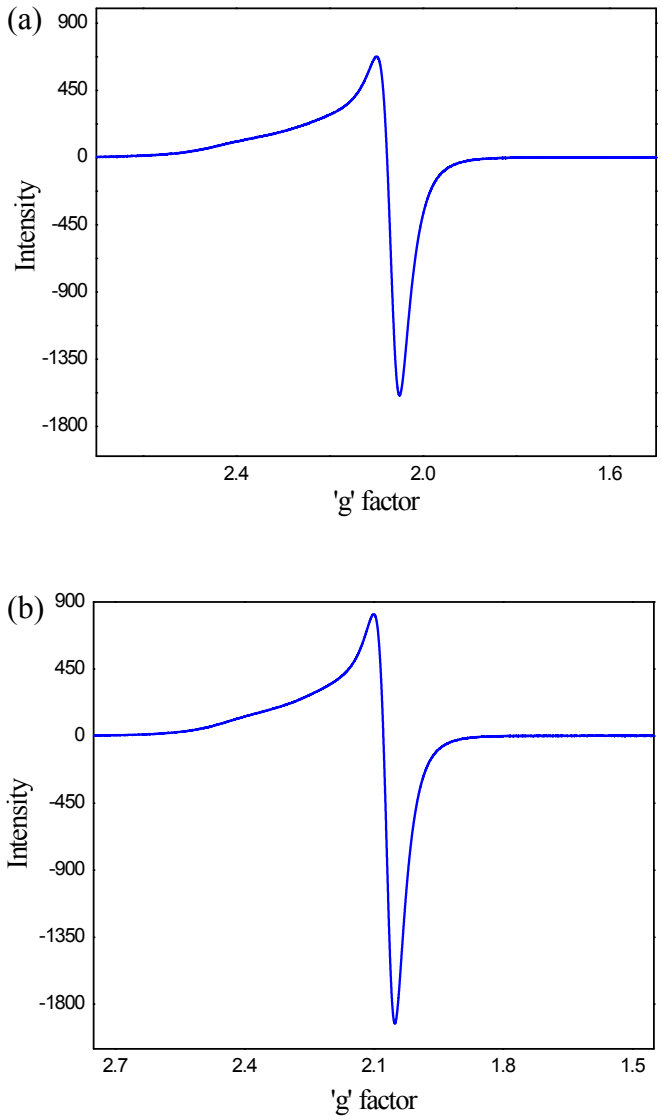

Fig. S6 Powder X-band EPR spectra of complexes 1 (a) and 6 (b).

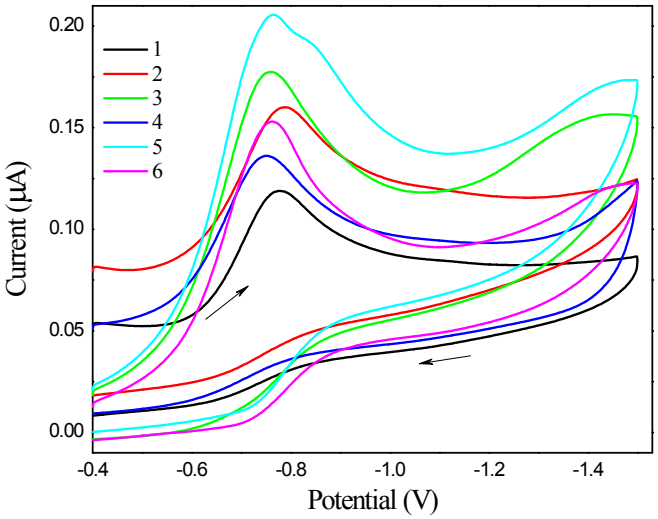

Fig. S7 Cyclic voltammograms of mixed–ligand copper(II) complexes (1–6) in the cathodic region.

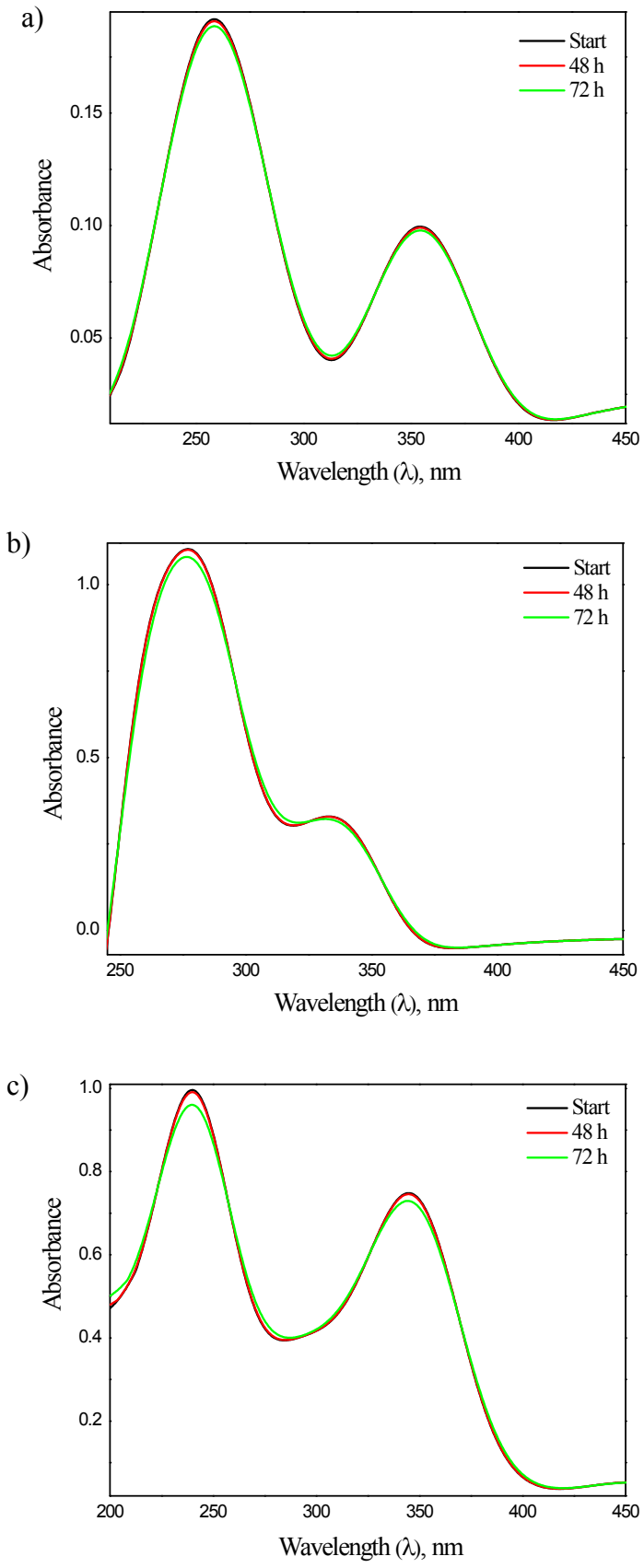

Fig. S8 Stability of complexes 1 (a), 5 (b) and 6 (c) measured by UV–Vis spectroscopy.

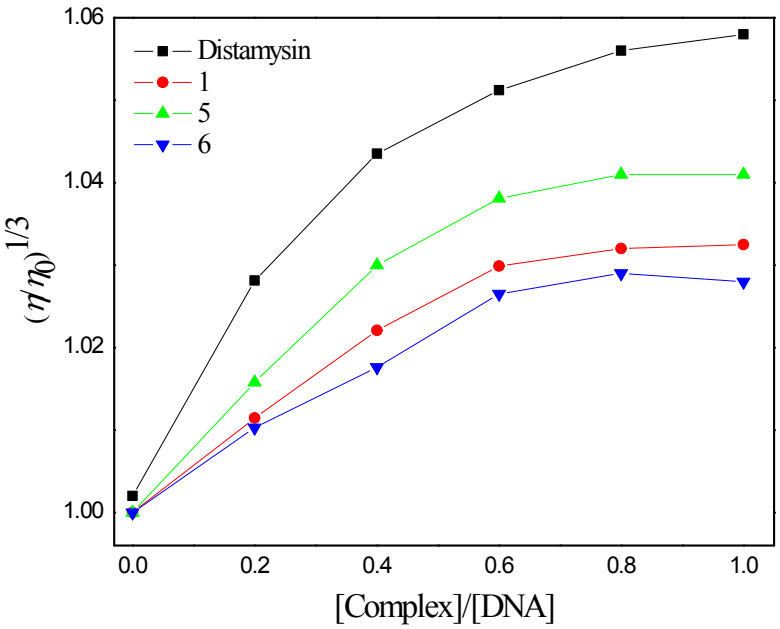

Fig. S9 Effect of complexes 1, 5 and 6 on the viscosity of CT–DNA. Relative specific viscosity *versus* 1/*R* (*R* = [DNA]/[Complex], [DNA] = 200 μM, [Complex] = 10–100 μM).

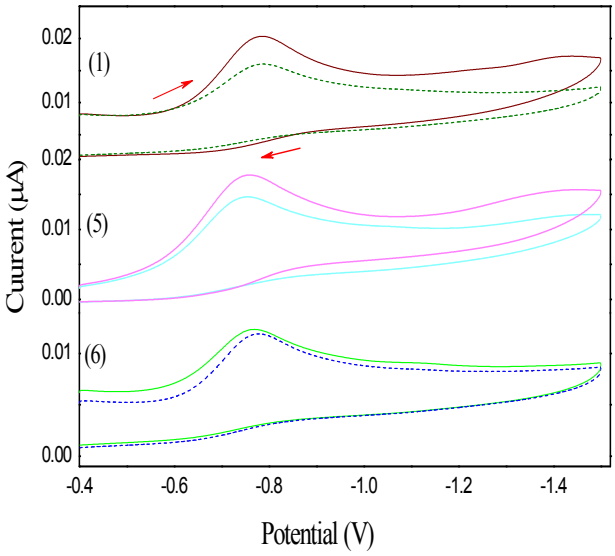

Fig. S10 Cyclic voltammograms of complexes 1, 5 and 6 in DMF–Tris–HCl/NaCl buffer at pH 7.3 in the absence (solid line) and presence (dotted line) of CT–DNA and arrow mark indicates the current changes upon increasing DNA concentration.

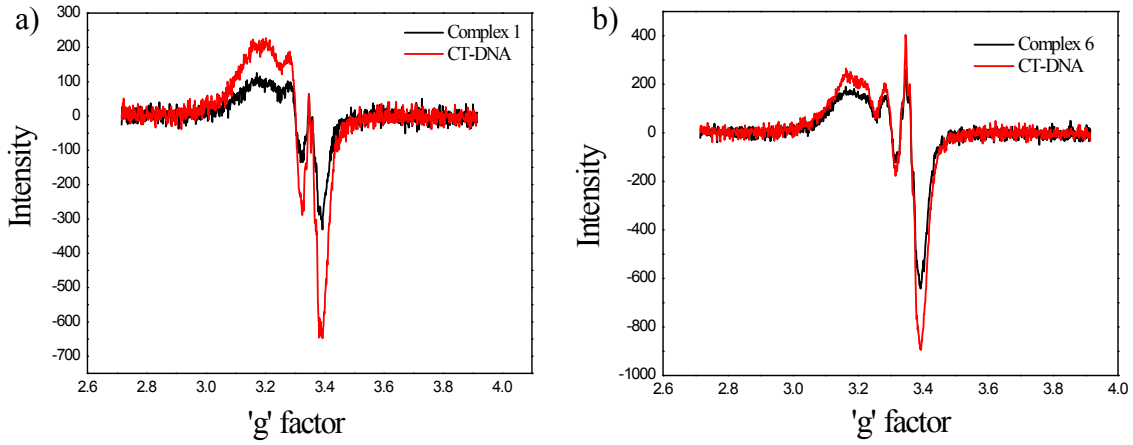

Fig. S11 EPR spectra of complexes 1 (a) and 6 (b) (25 µM) after 24 h incubation with CT–DNA (100 µM) at room temperature.

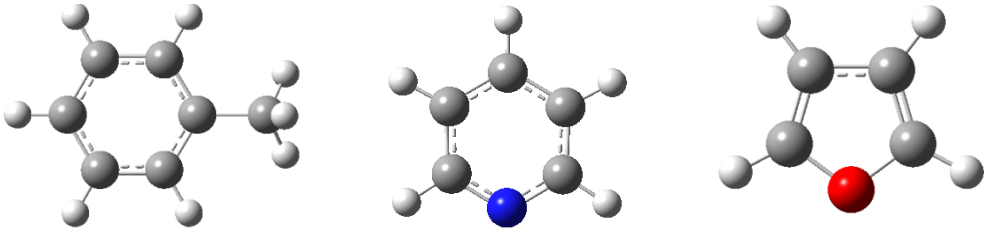

R1 R5 R6

Fig. S12 Optimized molecular structures of R1 (tolyl), R5 (pyridyl) and R6 (furyl) obtained from Gaussian 03W at the B3LYP/6-31G* level of calculation.